Available online at www.sciencedirect.com
SCIENCE DIRECT®
Journal of Hydrology 292 (2004) 296–307
Journal of Hydrology
www.elsevier.com/locate/jhydrol

Measuring catchment-scale chemical retardation using spectral analysis of reactive and passive chemical tracer time series

Xiahong Feng[a,*], James W. Kirchner[b], Colin Neal[c]

[a]Department of Earth Sciences, Dartmouth College, 6105 Sherman Fairchild Hall, Hanover, NH 03755-3571, USA
[b]Department of Earth and Planetary Science, University of California, 307 McCone Hall, Berkeley, CA 94720-4767, USA
[c]Center for Ecology and Hydrology, McLean Building, Wallingford, Oxon OX10 8BB, UK

Received 28 August 2002; revised 14 January 2004; accepted 29 January 2004

Abstract

Catchment-scale chemical transport is jointly controlled by hydrological and chemical processes. Water may take a complex set of flowpaths underground toward the stream, carrying soluble substances with it. Some chemical constituents are non-reactive; these act as passive tracers, moving with the water. Other constituents react with the porous medium; concentrations of these reactive tracers reveal how porewaters chemically interact with the subsurface. Thus, passive and reactive chemical tracers are indispensable tools for understanding hydrological and chemical processes at whole-catchment scale.

Transport of reactive chemical species can be quantified by the retardation factor, which measures the transport velocity of a reactive solute relative to the fluid that carries it. Retardation factors are conventionally determined by batch or column experiments involving small volumes of porous media. However, the transport media in typical catchments are highly heterogeneous, so retardation factors measured on small samples cannot be straightforwardly scaled up to model chemical transport at the catchment scale. Here, a novel method for determining whole-catchment retardation factors is presented which compares the power spectra of atmospherically derived passive and reactive tracers in rainfall and stream water. Using this technique, whole-catchment retardation factors of 2.4–2.9 were determined for sodium in four small catchments at Plynlimon, Wales. Because the effective retardation factor of a catchment depends on the degree of bypassing by preferential flow, our method for quantifying whole-catchment chemical retardation is of particular use for studying flowpaths and flow mechanisms at catchment scale.

Keywords: Solute transport; Tracers; Spectral analysis; Time series analysis; Catchments; Watersheds

1. Introduction

Subsurface transport processes control the delivery of chemical weathering products, atmospheric pollutants, and non-point-source contaminants to streams. Understanding these processes is critical for assessing how water quality will respond to natural and anthropogenic perturbations. However, quantifying transport processes at whole-catchment scale remains challenging, because of the complex and variable nature of fluid flowpaths and chemical reaction mechanisms. Some solutes are non-reactive and therefore act as passive tracers, moving with

* Corresponding author.
E-mail addresses: xiahong.feng@dartmouth.edu (X. Feng), kirchner@seismo.berkeley.edu (J.W. Kirchner), cn@ceh.ac.uk (C. Neal).

0022-1694/$ - see front matter © 2004 Elsevier B.V. All rights reserved.
doi:10.1016/j.jhydrol.2004.01.012

the water as it advects and disperses in the subsurface. Other solutes react with the substrate as the water flows through it. Hence, predicting the transport of these reactive solutes requires understanding not only subsurface advection and dispersion rates, but reaction characteristics (e.g. specific sorption) as well. The average transport rates of reactive chemical species are typically slower than those of passive species, because, at any given time, a portion of the reactive tracer is immobilized by sorption on the surface of the porous medium. This phenomenon of 'retarded' transport is quantified by the retardation factor, R_d (Bouwer, 1991; Freeze and Cherry, 1979; Vermeulen and Hiester, 1952), which is the ratio between the mean velocity of the water to the mean velocity of a reactive solute that it carries. Retardation factors are conventionally measured using small volumes of porous media collected at various locations within the catchment. Such point measurements do not reflect the fact that the catchment may be highly heterogeneous, and different parts of the subsurface medium may deliver different water and chemical fluxes (e.g. preferential flow). Therefore, it is difficult to use conventionally measured retardation factors to predict transport of solutes at whole-catchment scale, and thus to predict stream water quality.

Kirchner et al. (2000) studied detailed time series of chloride concentrations in rain and stream water at Plynlimon, Wales, and showed that chloride fluctuations in stream water are significantly damped compared to those in rainwater, indicating significant mixing in the subsurface. Their spectral analysis showed that chloride fluctuations in rainwater scale as white noise, whereas chloride fluctuations in streamwater scale as $1/f$ noise, except at timescales of many months or longer. Using this input–output spectral relationship of Cl fluctuations, they were able to determine the travel-time distribution of rainwater reaching the stream (assuming Cl to be non-reactive). More recently, Kirchner et al. (2001) showed that this $1/f$ scaling of Cl spectra was consistent with a simple model of downslope transport by advection and dispersion of spatially distributed rainfall Cl inputs. For reactive solutes that are retarded by their chemical interaction with the medium, the transport time to the stream would be longer than for a passive tracer like Cl. By comparing the travel-time distribution of a reactive and a passive tracer, it is possible to estimate the retardation factor of the reactive tracer at the whole-catchment scale. In this paper, we add chemical retardation to the downslope transport model of Kirchner et al. (2001), examining how the scaling behavior and travel-time distribution of a reactive tracer (Na) differ from those of a passive tracer (Cl). We determine the whole-catchment retardation factor for Na by comparing its power spectrum with that of Cl.

2. Retardation factor

We consider the simplest reaction system: a reactive tracer that undergoes equilibrium exchange via linear adsorption/desorption reactions between the aqueous phase flowing through the subsurface and an adsorbed phase on the medium through which the fluid flows. In such a system, the retardation of the reactive tracer relative to the fluid is quantified by the retardation factor (Bouwer, 1991; Freeze and Cherry, 1979; Vermeulen and Hiester, 1952)

$$R_d = 1 + \rho_b k_d/\theta \tag{1}$$

where ρ_b is the dry bulk density of the porous medium, and θ is its volumetric water content (for saturated media, θ is conventionally replaced by the porosity n). The parameter k_d is the equilibrium partition coefficient of the species between the adsorbed and aqueous phases

$$k_d = c_x/c \tag{2}$$

where c_x (μmol/g) and c (μmol/cm^3) are the concentrations of the tracer in the solid (or adsorbed) and aqueous phases, respectively. By combining Eqs. (1) and (2), one can see that R_d is the total mass of the tracer in the aqueous and adsorbed phases combined, divided by the mass in the aqueous phase alone. For a passive tracer, these two masses are equal (because the adsorbed mass is zero) and thus R_d is 1, whereas for reactive tracers R_d is greater than 1.

Solutes undergoing one-dimensional advection and dispersion in the subsurface and equilibrium adsorption/desorption reactions obey a simple advection–dispersion equation, rescaled for

retardation as follows

$$R_d \frac{\partial c}{\partial t} = D \frac{\partial^2 c}{\partial x^2} - v \frac{\partial c}{\partial x} \quad (3)$$

where t is time, v is the advection velocity of the fluid, D is the dispersion coefficient, and x is distance downstream along the flowpath. Predicting reactive tracer transport in the subsurface requires an estimate for R_d, but estimating retardation factors at catchment scale is difficult because of the highly heterogeneous character of typical catchments. One way to estimate R_d is to determine k_d using batch adsorption/desorption experiments and then calculate R_d using Eq. (1) (e.g. Hölttä et al., 2001). R_d can also be estimated from tracer transport experiments in packed columns in the laboratory (e.g. Maraqa, 2001). Solutions containing both reactive and passive tracers are applied at one end of the column and their breakthrough curves are measured at the other end. These measured breakthrough curves are then compared to the predictions of a simple one-dimensional model (such as Eq. (3)). Calibrating the model to the measured breakthrough curves yields parameter estimates for D, v, and R_d; the calibrated values of D and v are constrained to be identical for reactive and passive tracers alike, because they are all transported in the same solution.

However, neither batch experiments nor column experiments are likely to provide reliable estimates of whole-catchment chemical retardation, because they cannot capture the physical and chemical heterogeneity that is present at catchment scale. Here, we propose a novel method for measuring the retardation factor at catchment scale by comparing the power spectra of reactive and passive tracer concentrations in rainfall and stream water. We use Cl and Na time-series data from the Plynlimon catchments to demonstrate the method.

3. The Plynlimon catchments and relevant observations

The Plynlimon catchments have been described in a number of publications (e.g. Durand et al., 1994; Neal et al., 1997; Reynolds et al., 1986). Here, we summarize only those features that are relevant to this work. Data used for this work were obtained from samples collected from the Hafren, Tanllwyth, Upper Hore and Hore catchments, which are tributaries of River Severn in mid-Wales (Fig. 1). Rainfall and stream water samples were taken weekly for 9–17 years (depending on the catchment) as part of a long-term water quality monitoring study.

Several aspects of Na and Cl variations in rainfall and in stream water are important for this work. First, almost all of the Na at the Plynlimon catchments is,

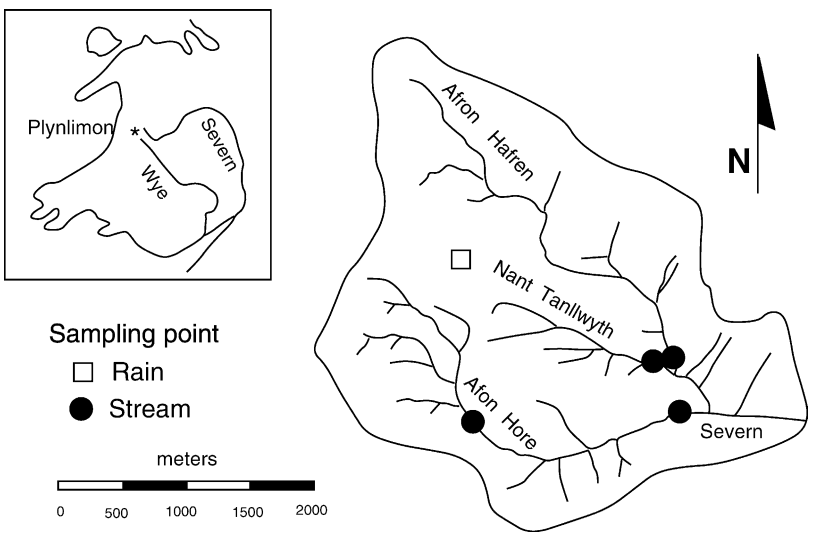

Fig. 1. Map of Plynlimon catchments and sampling points.

Table 1
Volume-weighted Na and Cl at Plynlimon

Stream	Area (km^2)	Years of record	Cl (μM)	Na (μM)	Na/Cl ratio	Fraction of Na from seasalt (%)
Hafren	3.5	17	199	179	0.899	96
Upper Hore	1.8	16	216	177	0.821	105
Hore	3.4	17	205	174	0.847	101
Tanllwyth	0.5	9	238	201	0.845	102
Rainfall		17	127	103	0.816	105

like Cl, derived from atmospheric deposition of seasalts. Input of Na from chemical weathering of the bedrock is insignificant compared to the seasalt deposition flux. This can be demonstrated by comparing the volume-weighted concentrations of Na and Cl in rainfall and streamflow (Table 1). Compared to the seasalt Na/Cl ratio of 0.859, the Na/Cl ratios of Plynlimon precipitation and streams range from 0.816 to 0.899. These ratios imply that 96–105% of Na in rainfall and streamflow at Plynlimon is derived from seasalt. This indicates that seasalt is the dominant source of Na in deposition and all of our study streams. Second, as mentioned earlier, Cl fluctuations in stream water are damped compared to the Cl fluctuations in rainfall. Neal and Kirchner (2000) showed that Na is even more strongly damped, and they suggested that the additional damping of Na relative to Cl is due to cation exchange buffering of Na by the catchment soils. Figs. 2 and 3 show this observation graphically. The Cl and Na time series show that Cl concentrations are more variable than Na concentrations, not only in the weekly raw data, but also in 90-day and annual averages as well

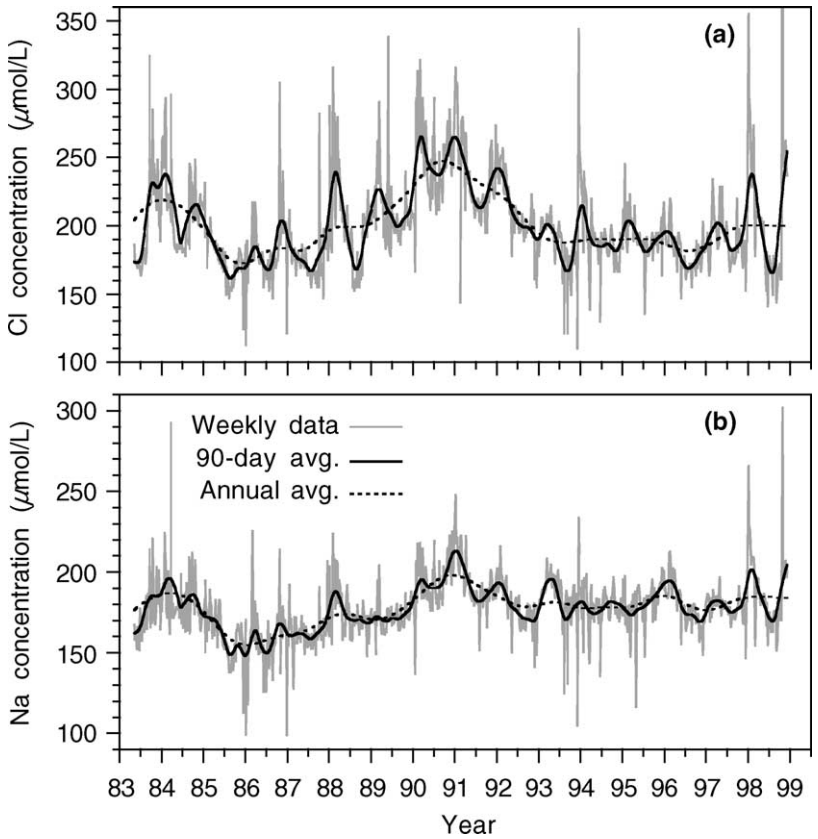

Fig. 2. Time series of Cl and Na concentrations in Hafren stream. The Cl axis has been compressed relative to the Na axis by the seasalt ratio (0.859), so Na and Cl would appear equally variable if seasalt fluctuations of Na and Cl were transmitted equally through the catchment. Instead, however, Na is less variable than Cl for the weekly observations as well as for 90-day and annual averages.

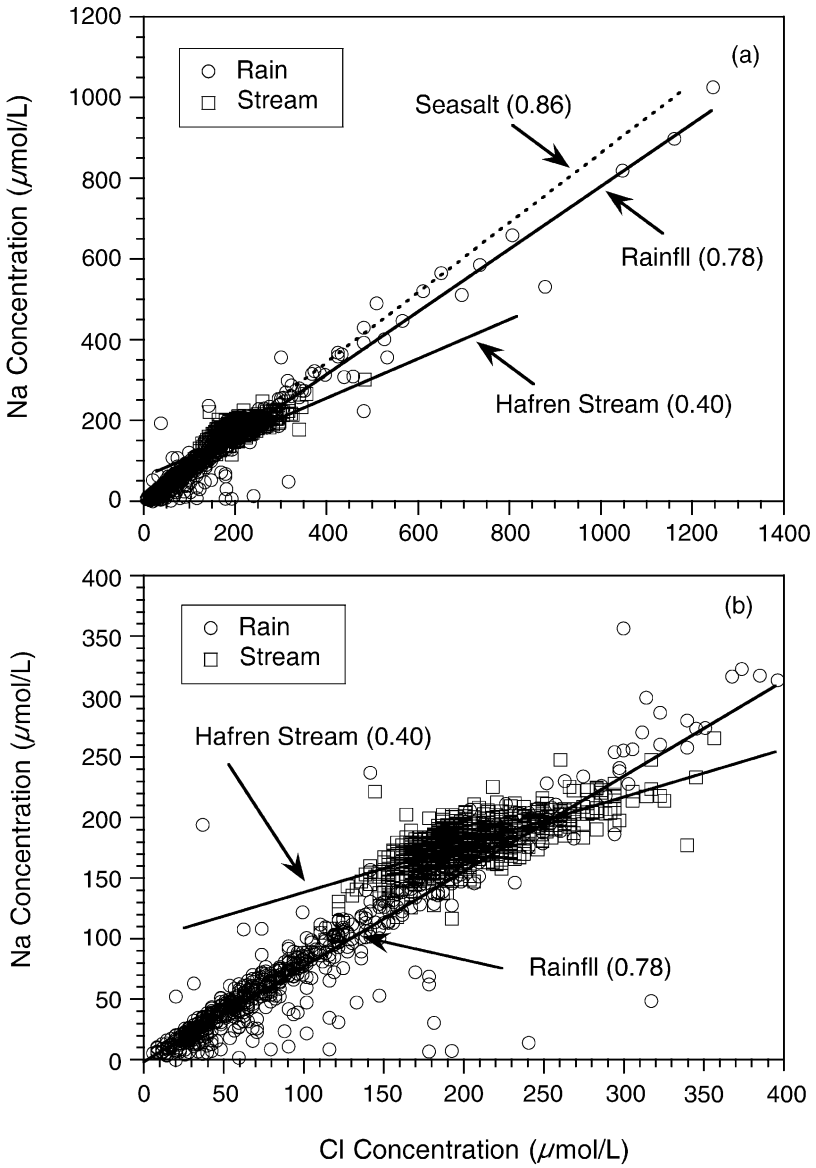

Fig. 3. Na against Cl for rainfall and stream water at Hafren over the full concentration range (a), and over a low concentration range (b). The seasalt ratio of 0.86 is shown in (a) as a reference. Na and Cl are significantly correlated for both rainfall and stream samples; the regression slopes are shown in parentheses. The intercept of the Na–Cl regression line in rainfall water is close to zero (0.3 ± 1.2 μmol/l) and, therefore, the slope represents the Na/Cl ratio. This ratio (0.78) is only slightly lower than the seasalt ratio. The slope of the Na–Cl regression line for stream water is 0.40, lower than the seasalt ratio by a factor of two. The different slopes in rainfall and stream samples are shown more clearly in (b). When Cl concentrations are high, Na concentrations are lower than predicted by the seasalt ratio, and vice versa. This suggests that Na concentrations are buffered by cation exchange within the catchment (Neal and Kirchner, 2000).

(Fig. 2). Note that in Fig. 2, the Cl axis has been compressed relative to the Na axis by a proportion equal to the seasalt ratio (0.859). Plotted this way, Na and Cl would appear equally variable if seasalt fluctuations of Na and Cl were transmitted equally through the catchment. Instead, Na is more strongly damped than Cl, on all timescales from weeks to years (Fig. 2). Fig. 3 is a plot of Na concentration against Cl

concentration for one of the sampled streams (Hafren). The slope of Na vs. Cl for rainfall is 0.78, only slightly lower than the Na/Cl ratio of seasalt, while the slope for stream water is 0.4. When the Cl concentration is high, the Na concentration is lower than predicted by the seasalt ratio, and vice versa; this pattern of behavior is consistent with damping of Na by cation exchange (Neal and Kirchner, 2000). Other streams at Plynlimon exhibit similar behavior. Finally, the power spectra of Na and Cl also indicate the effect of cation exchange on Na transport. Fig. 4 shows the power spectra of Cl and Na for rainfall and stream water. Before computing the spectra shown in Figs. 4 and 6, we multiplied the Na concentration data by $1/0.859 = 1.164$, the inverse of the Na/Cl seasalt ratio. This makes seasalt fluctuations of Na and Cl equal in amplitude; thus, the spectral power of seasalt-adjusted Na and Cl will be the same if they are varying solely due to fluctuations in seasalt inputs (the same effect could be achieved by multiplying the Na power spectrum by $1/0.859^2 = 1.355$). Fig. 4 shows that, as expected, the rainfall spectrum is about the same for Na and Cl, scaling roughly as white noise.

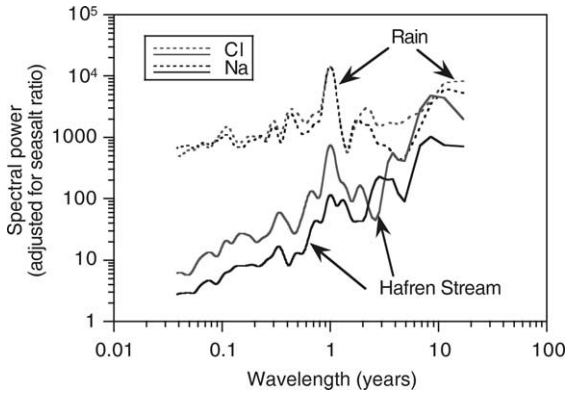

Fig. 4. Power spectra of Cl and Na variations in rainfall and stream water. Na spectra are calculated from Na concentrations multiplied by $1/0.859 = 1.164$, the reciprocal of the Na/Cl seasalt ratio; adjusting Na in this way makes the spectral power of Na equal to that of Cl for variations that are solely due to fluctuations in seasalt inputs. Cl and Na variations in rainfall scale roughly as white noise and have the same power. The spectral power of Cl variations in streamwater is lower than in rainfall, with the difference increasing with decreasing wavelength. This indicates that the high-frequency fluctuations of Cl in rainfall are damped by transport and mixing in the catchment. The spectral power of Na in stream water is further depressed relative to Cl across the range of wavelengths analyzed, indicating that seasalt fluctuations of Na are more strongly damped than Cl.

The spectrum of Cl in streamflow scales approximately as $1/f$ noise (Kirchner et al., 2000). The damping of streamflow Cl relative to rainfall Cl increases systematically with decreasing wavelength, reflecting transport and mixing of rainfall inputs on many timescales. The power spectrum of Na in streamwater has the same scaling behavior as that of Cl (the two spectra are parallel in trend), but its power is systematically lower. Thus, Na fluctuations in streamwater are damped relative to Cl across the range of timescales analyzed, implying that Na fluctuations are damped not only by subsurface transport and mixing, but by chemical mechanisms as well.

4. Determination of R_d at catchment scale

Using the power spectra of passive tracers such as Cl in rainfall and streamflow, one can infer the travel-time distribution linking rainfall and streamflow at catchment scale (Kirchner et al., 2000). We have previously shown that the spectral characteristics of Cl at Plynlimon are consistent with a simple one-dimensional model of subsurface transport by advection and dispersion (Kirchner et al., 2001). Here, we briefly review this approach, and show how it can be extended to estimate the catchment-scale retardation factor for reactive solutes.

4.1. Travel-time distributions of chemical tracers

The catchment-scale travel-time distribution for a chemical tracer expresses the fraction of today's chemical deposition that will reach the stream today, tomorrow, the day after tomorrow, and so forth. The travel-time distribution of a passive chemical tracer should be the same as the travel-time distribution of the water that carries it. A reactive tracer's travel-time distribution, by contrast, will be stretched out by chemical retardation.

For a chemical tracer that is supplied to the catchment entirely by rainfall, the concentration in the stream $c_S(t)$ at any time t will be the convolution of the travel-time distribution $h(\tau)$ and the rainfall concentration at all previous times $c_R(t - \tau)$, where

τ is the lag time between rainfall and runoff:

$$c_S(t) = \int_0^\infty h(\tau) c_R(t-\tau) d\tau \quad (4)$$

Because the flow rate varies through time, Eq. (4) is strictly valid when t and τ are expressed in terms of the cumulative flow through the catchment, rather than calendar time (Neimi, 1977; Rodhe et al., 1996), but the mathematics are the same in either case (Neimi, 1977). Eq. (4) implies that if the tracer input $c_R(t-\tau)$ is a delta function (a brief, sharp pulse), the travel-time distribution $h(\tau)$ can be estimated directly from the tracer output time series $c_S(t)$. Likewise, if the tracer input $c_R(t-\tau)$ is a step function, Eq. (4) implies that the travel-time distribution can be estimated from the derivative of the tracer output time series $c_S(t)$. This is why laboratory column experiments typically use pulse or step inputs; they make the calculation of $h(\tau)$ and other transport parameters relatively straightforward.

By contrast, naturally occurring environmental tracers typically have complicated input time series, making it impossible to estimate their travel-time distributions directly from Eq. (4). However, even noisy time series can be used to constrain the travel-time distribution $h(\tau)$ by employing the convolution theorem, which states that the convolution expressed by Eq. (4) is equivalent to multiplying the Fourier transforms of each of its terms

$$C_S(f) = H(f) C_R(f) \quad \text{and} \quad |C_S(f)|^2 = |H(f)|^2 |C_R(f)|^2 \quad (5)$$

where f is frequency (cycles/time); $C_S(f)$, $H(f)$, and $C_R(f)$ are the Fourier transforms of $c_S(t)$, $h(\tau)$, and $c_R(t-\tau)$; $|C_S(f)|^2$, $|H(f)|^2$, and $|C_R(f)|^2$ are their power spectra (Gelhar, 1993).

A tracer input time series c_R can be viewed as many different cycles on many different wavelengths, superimposed on one another. The convolution in Eq. (4) implies that if one of these component cycles in c_R fluctuates on a wavelength that is short compared to the travel-time distribution $h(\tau)$, waters with high and low tracer concentrations will be mixed together in the stream, and the fluctuation in the stream will therefore be damped relative to the input. The more rapid the fluctuation in the input compared to the travel-time distribution, the greater this attenuation by averaging will be. Conversely, components of c_R that fluctuate on wavelengths that are long compared to the travel-time distribution will be transmitted with little attenuation.

Eq. (5) formalizes this intuitive picture, and quantifies the damping of tracer fluctuations (from rainfall to streamflow) by the ratio of their spectral power. Thus, Eq. (5) allows one to test alternative travel-time models $h(\tau)$ by calculating their power spectra $|H(f)|^2$, and testing whether they are consistent with the relationship between the input and output power spectra $|C_R(f)|^2$ and $|C_S(f)|^2$. Kirchner et al. (2001) showed that the Plynlimon power spectra were consistent with a simple model of downslope advection and dispersion (defined in Eq. (3) with $R_d = 1$) of spatially distributed rainfall inputs (see Fig. 5). In this work, we add chemical retardation to this model, and show that the retardation factor R_d can be estimated straightforwardly by comparing the input and output spectra for a reactive tracer and a passive tracer.

4.2. The advection–dispersion model for tracer transport

Kirchner et al.'s (2001) model is based on a simple thought experiment that considers a hillslope cross-section, in which water flows along a one-dimensional hillslope through a shallow subsurface layer. Here, 'shallow' means only that the thickness of the conducting layer is much less than the hillslope length L; this layer may include both soil and weathered or fractured bedrock, and we make no specific assumption concerning where subsurface flow occurs in this conducting layer. We assume that bulk advection through this layer occurs at a fixed velocity v, determined by the hydraulic conductivity of the medium and the slope of the underlying impermeable layer. We then consider how a pulse of chemical tracer in rainfall will be transported downslope, if the tracer undergoes advection, dispersion, and retardation as specified in Eq. (3).

If a pulse of tracer is introduced at a single point, at a distance l from the stream channel, the distribution of its arrival times τ at the stream channel will be

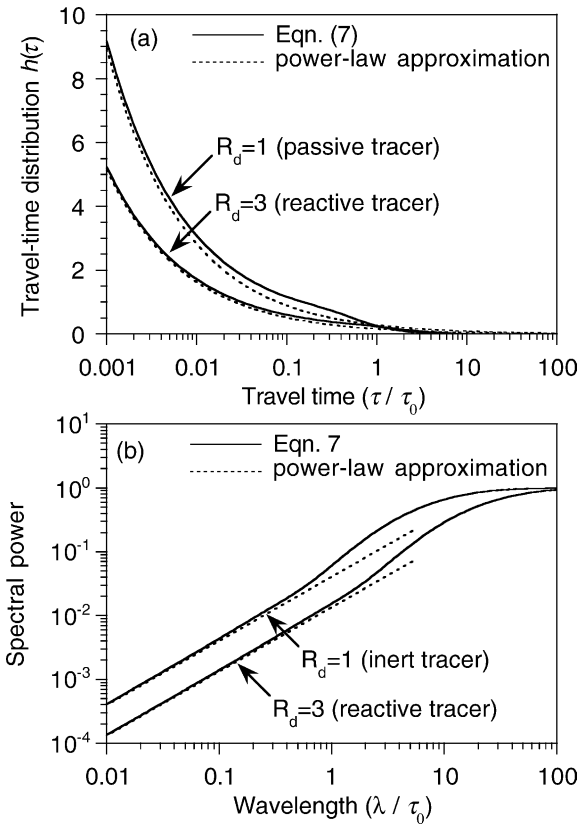

Fig. 5. The upper panel shows travel-time distributions for downslope advection and dispersion of spatially distributed inputs (Eq. (7)) for a non-sorbing tracer ($R_d = 1$) and a sorbing tracer (here, $R_d = 3$). The dotted lines show power-law approximations (Eq. (9)) to the short-time part of the travel-time distributions. The lower panel shows the power spectra for the two travel-time distributions, computed from Eq. (7) by Fourier integration. The dotted lines show the power spectra (Eq. (10)) of the power-law approximations to the travel-time distributions. Plots shown here are for $Pe = 1$; plots for $Pe \approx 1$ or less are qualitatively similar. The power spectra of the travel-time distributions are almost indistinguishable from those of the power-law approximations at wavelengths shorter than $PeR_d\tau_0$ (corresponding to $\lambda/\tau_0 < 1$ for $R_d = 1$ and $\lambda/\tau_0 < 3$ for $R_d = 3$ in these plots). In these wavelength ranges, the effect of chemical retardation is to diminish the spectral power by a factor of R_d.

(following Kreft and Zuber, 1978):

$$p(l,\tau) = \frac{l}{\sqrt{4\pi D\tau^3/R_d}} e^{-(l-v\tau/R_d)^2/(4D\tau/R_d)} \quad (6)$$

Tracer pulses that land close to the stream will reach it quickly, and will undergo relatively little dispersion; tracer pulses that land farther upslope will arrive at the stream later and will undergo more dispersion. The tracer signal in the stream will be the integral of the contributions from each point along the length of the hillslope. To obtain the travel-time distribution for the entire hillslope, we need to integrate Eq. (6) from the channel ($l = 0$) to the divide ($l = L$). This integral yields:

$$\begin{aligned} h(\tau) &= \int_{l=0}^{L} p(l,\tau)\mathrm{d}l \\ &= \frac{1}{L}\sqrt{\frac{D/R_d}{\pi\tau}}\left[e^{-(-v\tau/R_d)^2/(4D\tau/R_d)} - e^{-(L-v\tau/R_d)^2/(4D\tau/R_d)}\right] + \frac{v/R_d}{2L} \\ &\quad \times\left[\mathrm{erf}\left(\frac{L - v\tau/R_d}{\sqrt{4D\tau/R_d}}\right) - \mathrm{erf}\left(\frac{-v\tau/R_d}{\sqrt{4D\tau/R_d}}\right)\right] \end{aligned} \quad (7)$$

We can condense Eq. (7) by re-expressing it in terms of the Peclet number $Pe = vL/2D$ (the ratio of advective to dispersive mass transport), and the mean travel-time for the water, $\tau_0 = L/2v$.

$$\begin{aligned} h(\tau) &= \sqrt{\frac{1}{4\pi Pe\tau R_d\tau_0}} e^{-Pe\tau/4R_d\tau_0}\left[1 - e^{(z_0)^2-(z_L)^2}\right] \\ &\quad + \frac{1}{4R_d\tau_0}\left[\mathrm{erf}(z_L) - \mathrm{erf}(z_0)\right], \end{aligned} \quad (8)$$

where

$$z_0 = -\frac{1}{2}\sqrt{Pe\tau/R_d\tau_0} \qquad \text{and}$$

$$z_L = \sqrt{PeR_d\tau_0/\tau} - \frac{1}{2}\sqrt{Pe\tau/R_d\tau_0}$$

Kirchner et al. (2001) showed that this advection–dispersion model was consistent with the power spectrum of the chloride tracer (assuming $R_d = 1$) at Plynlimon, as long as the Peclet number is roughly of order 1 or smaller. Within this range of Pe, the shape of the spectrum for Eq. (8) is not sensitive to the value of Pe. Values of $Pe \approx 1$ imply that the dispersivity length scale is on the same order as the mean subsurface path length (i.e. half the hillslope length), and thus that the subsurface flow system exhibits strong heterogeneity up to and including this scale (Kirchner et al., 2001). However, the chloride tracer spectra do not provide an empirical constraint on the nature of this flow system or its conductivity contrasts (e.g. pipeflow vs. fracture flow).

4.3. Determination of R_d

For a given catchment, all chemical tracers share the same Peclet number because they are all transported in the same water and the same medium. We can explore the effect of R_d on the travel-time distribution and its power spectrum using the following approximation. For $Pe \approx 1$ or less and $\tau \ll PeR_d\tau_0$, Eq. (7) is closely approximated by its leading term

$$h(\tau) \approx \sqrt{\frac{1}{4\pi Pe\tau R_d\tau_0}} = \sqrt{\frac{D}{\pi L^2 R_d \tau}} \tag{9}$$

As Fig. 5 shows, this power-law approximation conforms closely to the short-time behavior of the full travel-time distribution. We can use this to advantage, because the short-wavelength part of the power spectrum (which is what can be measured most accurately from data) is determined almost entirely by the short-time portion of the travel-time distribution. Thus, at wavelengths less than $PeR_d\tau_0$, the power spectrum of the travel-time distribution (Eq. (7)) is closely approximated by the spectrum of the power-law approximation (Eq. (9)), which is:

$$|H(f)|^2 \approx \frac{1}{8\pi PeR_d\tau_0 f} = \frac{D}{2\pi L^2 R_d f} \tag{10}$$

for $f > 1/PeR_d\tau_0$

Fig. 5 shows that this approximation is almost indistinguishable from the power spectrum of Eq. (7) for wavelengths less than $PeR_d\tau_0$ (or $\lambda/\tau_0 < 1$ for $R_d = 1$ and $\lambda/\tau_0 < 3$ for $R_d = 3$ in these plots in Fig. 5b). Note that in this wavelength range, spectral power is inversely proportional to R_d. Thus, we can estimate R_d from the ratio between the high-frequency spectra of a passive tracer and a reactive tracer. From Eqs. (10) and (5), we obtain directly:

$$\frac{(R_d)_{Na}}{(R_d)_{Cl}} \approx \frac{|H(f)|^2_{Cl}}{|H(f)|^2_{Na}} = \frac{|C_S(f)|^2_{Cl}}{|C_S(f)|^2_{Na}} \frac{|C_R(f)|^2_{Na}}{|C_R(f)|^2_{Cl}} \tag{11}$$

for $f > 1/PeR_d\tau_0$

We can simplify this approach in two ways. First, we assume Cl is non-reactive and thus $R_d = 1$ for Cl. Second, if Na and Cl fluctuations in deposition are dominated by variations in the amount of seasalt, and we adjust the concentration of Na or Cl by the Na/Cl seasalt ratio (as in Fig. 4 above), then $|C_R(f)|^2_{Na} \approx |C_R(f)|^2_{Cl}$. With these simplifications, Eq. (11) becomes:

$$(R_d)_{Na} \approx \frac{|C_S(f)|^2_{Cl}}{|C_S(f)|^2_{Na}} \qquad \text{for } f > 1/PeR_d\tau_0 \tag{12}$$

Eq. (12) shows that R_d can be estimated from the vertical offset between the Cl and Na spectra on a log–log plot.

Fig. 6 shows the average offsets between the Cl and Na spectra for four Plynlimon streams. These offsets yield the catchments' average $(R_d)_{Na}$ values, which vary relatively little, ranging from 2.4 at Upper Hore to 2.6 at Tanllwyth, 2.7 at Hafren, and 2.9 at Hore. Fig. 7 shows the $(R_d)_{Na}$ values calculated at each frequency for each stream. The results show that estimates of $(R_d)_{Na}$ are consistently in the range of 2–3.5 for all four streams, at wavelengths shorter than roughly 1 year.

5. Discussion

Our analysis shows that one can measure the whole-catchment retardation factor for reactive chemical species by comparing the power spectra of passive and reactive tracers in rainfall and streamflow in small catchments. This new method may provide a unique approach for studying chemical transport behavior and its relationship with hydrological processes in catchments. To our knowledge, retardation factors have not previously been reported for an entire catchment. Hölttä et al. (1997) estimated Na retardation factors for several geological materials by measuring the partition coefficient k_d (Eq. (2)). They reported $R_d = 2.3–5.2$ for a mica gneiss, $R_d = 3.1–50$ for altered tonalite, and $R_d = 1.4–5.4$ for fresh tonolite using a Na concentration of 240 μmol/l. This Na concentration is within the concentration range of the Plynlimon streams.

A solute's retardation factor depends in a complex way on its chemical behavior, the chemical characteristics of the medium through which it passes, the geometry of the pore network, and the hydrological

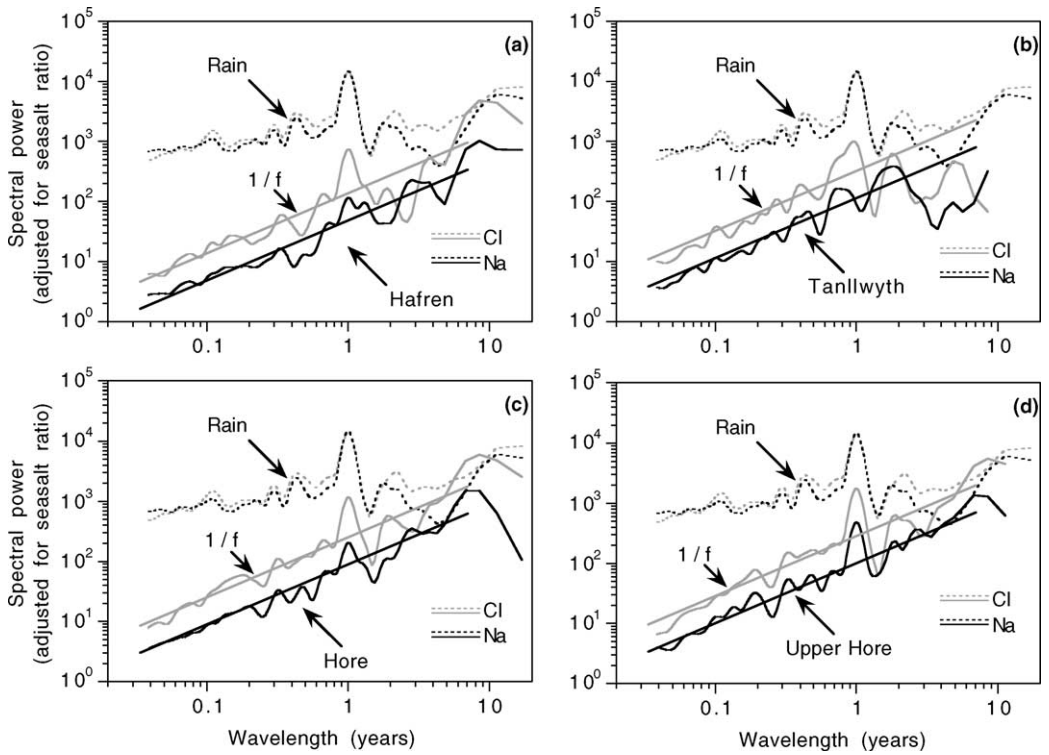

Fig. 6. Power spectra of sodium and chloride in rainfall and four streams at Plynlimon, Wales. The Na spectra are calculated from Na concentrations multiplied by 1/0.859 = 1.164, the reciprocal of the Na/Cl seasalt ratio; adjusting Na in this way makes the spectral power of Na and Cl equal for variations that are solely due to fluctuations in seasalt inputs. The systematic damping of Na relative to Cl in streamwater is consistent with whole-catchment retardation factors of $R_d = 2.7$, 2.6, 2.9, and 2.4 for Hafren, Tanllwyth, Hore, and Upper Hore, respectively.

conditions. As Eq. (1) makes clear, the retardation factor is inversely proportional to the water content θ (Bouwer, 1991). The 'effective' retardation factor observed at catchment scale should also be affected by the flow mechanism, e.g. whether the flow is piston flow or preferential flow. In the case of preferential flow, water does not flow through all pores, and therefore bypasses some fraction of the potential adsorption sites. Thus, the effective retardation may be lower for preferential flow than for piston flow in the same medium (Bouwer, 1991). More generally, the retardation factor may be affected by heterogeneity of the medium. More permeable areas or layers deliver more flux of water than relatively impermeable areas or layers. The permeable layers usually have smaller surface area per unit volume, and thus lower adsorption capacity, because the medium is usually coarser. Bouwer (1991) numerically

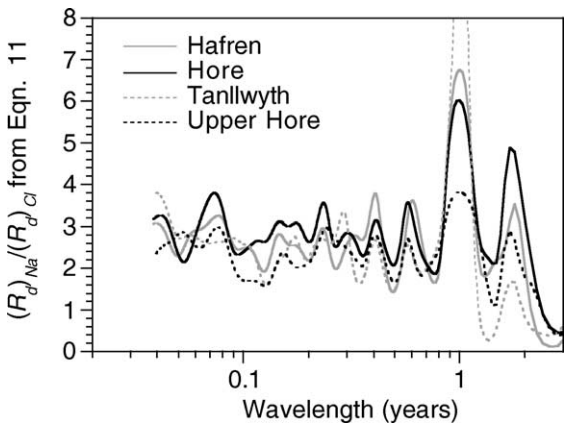

Fig. 7. Retardation of Na relative to Cl, estimated from rainfall and streamflow spectra via Eq. (11). Estimates of R_d are consistently in the range of 2–3.5 for all four streams at wavelengths shorter than roughly 1 year.

simulated a saturated medium in which four layers with different permeability were stacked together. The effective retardation factor of the entire unit was close to that of the most permeable layer. Our spectral estimation method yields a spatially and temporally averaged retardation factor that reflects any complications of this nature that may be present in an individual catchment. Thus, one should not expect R_d values obtained through our spectral estimation method to agree with those calculated from batch experiments or column experiments in the laboratory, or with those obtained from breakthrough curves measured along an individual flowpath within the catchment. For the same reason, laboratory measurements of the retardation factor may not provide reliable estimates of the effective catchment-scale retardation factor for modeling spatially heterogeneous catchments.

Because the retardation factor is affected by hydrological conditions, whole-catchment estimates of effective retardation factors are useful for studying catchment hydrological processes. For example, whole-catchment R_d values could be compared with R_d estimates for catchment media, calculated via Eq. (1) from measurements of k_d or estimated from column breakthrough experiments. If preferential flow bypasses a significant fraction of the catchment's solute adsorption capacity, the R_d determined by the spectral estimation method should be lower than the R_d determined from batch or column experiments. In this way, it may be possible to estimate how much of the catchment's subsurface media are bypassed by preferential flow, or even, with proper data, to estimate how the degree of bypassing by preferential flow differs between high flow and low flow.

Our spectral estimation method requires comparing tracer concentration fluctuations in both the catchment input and output. In practice, this means that both the passive and reactive tracers must be derived from atmospheric deposition, with no significant sources or sinks within the catchment (apart from the incremental adsorption and desorption that causes chemical retardation). This requirement is met at the Plynlimon catchments, where Na and Cl inputs are dominated by seasalt deposition. Our method may not be applicable to other catchments in which seasalt deposition fluxes are smaller, and weathering fluxes or biological uptake and release are relatively more important. Our method may also only be applicable to catchments that are small enough (≤ 10's of km^2) that strong deposition gradients do not complicate the analysis. These requirements may rule out all but a small fraction of catchments as candidates for this technique. However, even if these methods cannot be broadly applied, they nonetheless provide a unique opportunity to quantify hydrological and geochemical processes that are of broad significance to many diverse catchments.

6. Conclusions

At the Plynlimon catchments, Cl and Na are both predominantly derived from atmospheric deposition. The Na/Cl ratio in stream water is close to the seasalt ratio, indicating that weathering inputs of Na are insignificant. Both Cl and Na concentrations are much less variable in streamwater than in rainfall, with spectral power decreasing proportionally to wavelength, indicating that these catchments transport and mix rainfall inputs of Cl and Na across a wide range of timescales. The spectral power of Na in streamflow scales similarly to Cl but is systematically lower, indicating that Na varies less than Cl on timescales from weeks to decades. The additional damping of Na fluctuations relative to Cl is consistent with chemical retardation of Na by adsorption/desorption reactions within the catchments. This chemical buffering of Na fluctuations adds to the damping caused by advection and dispersion in the subsurface (which should damp fluctuations in Na and Cl equally).

The damping of Cl fluctuations from rainfall to streamflow can be explained by a simple model of advection and dispersion of spatially distributed rainfall Cl inputs (Kirchner et al., 2001). To account for the additional damping of Na by adsorption/desorption reactions, we incorporated chemical retardation into the advection/dispersion model of Kirchner et al. (2001). Analysis of this advection/dispersion/reaction model shows that the whole-catchment retardation factor can be measured from the vertical offset between the power spectra of Na and Cl (or more generally, from the power spectra of any reactive tracer and passive tracer for which input and output time series are available). For four catchments at Plynlimon, the whole-catchment

retardation factors for Na occupy a narrow range, from 2.4 to 2.9.

The retardation factor should vary with hydrological conditions in a catchment, including the degree of saturation and the extent of bypassing by preferential flow. By studying the chemical retardation of reactive tracers at whole-catchment scale, it may be possible to estimate how much of the catchment's subsurface media are bypassed by preferential flow and whether the extent of bypassing by preferential flow varies between high-flow and low-flow conditions.

Acknowledgements

Our collaboration was supported by National Science Foundation grants EAR-9903281, EAR-0125338 and EAR-0125550. Sample collection and analysis were supported by the Natural Environment Research Council, the Environment Agency of England and Wales, and the Forestry Commission. We thank the Plynlimon field staff for sample collection, M. Neal for sample analysis, and C. Renshaw for helpful discussions.

References

Bouwer, H., 1991. Simple derivation of the retardation equation and application to preferential flow and macrodispersion. Ground Water 29(1), 41–46.

Durand, P., Neal, C., Jeffery, H.A., Ryland, G.P., Neal, M., 1994. Major, minor and trace element budgets in the Plynlimon afforested catchments (Wales): general trends, and effects of felling and climate variations. Journal of Hydrology 157, 139–156.

Freeze, R.A., Cherry, J.A., 1979. Groundwater, Prentice-Hall, Englewood Cliffs, NJ.

Gelhar, L.W., 1993. Stochastic Subsurface Hydrology, Prentice-Hall, Englewood Cliffs, NJ.

Hölttä, P., Siitari-Kauppi, M., Hakanen, M., Huitti, T., Hautojarvi, A. Lindberg, A., 1997. Radionuclide transport and retardation in rock fracture and crushed rock column experiments. Contaminant Hydrology, 26: 135–145.

Hölttä, P., Siitari-Kauppi, M., Hakanen, M., Tukiainen, V., 2001. Attempt to model laboratory-scale diffusion and retardation data. Contaminant Hydrology 47, 139–148.

Kirchner, J.W., Feng, X., Neal, C., 2000. Fractal stream chemistry and its implications for contaminant transport in catchments. Nature 403, 524–527.

Kirchner, J.W., Feng, X., Neal, C., 2001. Catchment-scale advection and dispersion as a mechanism for fractal scaling in stream tracer concentrations. Journal of Hydrology 254, 82–101.

Kreft, A., Zuber, A., 1978. On the physical meaning of the dispersion equation and its solutions for different initial and boundary conditions. Chemical Engineering Science 33, 1471–1480.

Maraqa, M.A., 2001. Prediction of mass-transfer coefficient for solute transport in porous media. Journal of Contaminant Hydrology 53, 153–171.

Neal, C., Kirchner, J.W., 2000. Sodium and chloride levels in rainfall, mist, streamwater and groundwater at the Plynlimon catchments, mid-Wales: inferences on hydrological and chemical controls. Hydrology and Earth System Sciences 4(2), 295–310.

Neal, C., Wilkinson, J., Neal, M., Harrow, M., Wickham, H., Hill, S., Morfitt, C., 1997. The hydrochemistry of the headwater of the river Severn, Plynlimon. Hydrology and Earth System Sciences 1(3), 583–617.

Neimi, A.J., 1977. Residence time distributions of variable flow processes. International Journal of Applied Radiation and Isotopes 28, 855–860.

Reynolds, B., Neal, C., Hornung, M., Stevens, P.A., 1986. Baseflow buffering of streamwater acidity in five mid-Wales catchments. Journal of Hydrology 87, 167–185.

Rodhe, A., Nyberg, L., Bishop, K., 1996. Transit times for water in a small till catchment from a step shift in the oxygen 18 content of the water input. Water Resources Research 32(12), 3497–3511.

Vermeulen, T., Hiester, N.K., 1952. Ion exchange chromatography of trace elements. Industrial Engineering Chemistry 44, 636–651.